Stimulated Raman Scattering in Membrane Silicon Waveguides

F. De Leonardis[1] and V. M. N. Passaro[2]

[1]Photonics Research Group, Dipartimento di Ingegneria dell'Ambiente e per lo Sviluppo Sostenibile, Politecnico di Bari, Taranto, Italy
f.deleonardis@poliba.it
[2]Photonics Research Group, Dipartimento di Elettrotecnica ed Elettronica, Politecnico di Bari, Bari, Italy

Abstract. *An investigation and optimization of silicon rib-membrane waveguides for Stimulated Raman Scattering applications is presented.*

Introduction

In order to develop Silicon Photonics, main areas or building blocks for investigation include selectively guiding and transporting of the light within the silicon, encoding light, detecting light, amplification and generation the light, packaging the devices and intelligent control of these photonic functions. While a wide variety of passive devices were developed in the 1990's, recent activities have focused on achieving active functionality, mostly light amplification and generation, in silicon-on-insulator (SOI) waveguides. In particular, the approach for light generation based on Stimulated Raman Scattering (SRS) in SOI technology has recently met a large interest [1]. More recently, new silicon-based waveguides have been proposed to manage the propagation loss in the near and long-wave infrared region [2]. This work represents a first investigation of SRS effect in silicon membrane waveguides, demonstrating the possibility to increase the Raman amplification by an appropriate design of air membrane.

Theory

When Stokes optical pulses propagate inside a waveguide in sub-picosecond regime, both dispersive and nonlinear effects largely influence their shapes and spectra. Space-time evolution of Stokes waves can be described by the following equation:

$$\begin{aligned}
&\frac{\partial A_\kappa}{\partial z}+\beta_{1\kappa}\frac{\partial A_\kappa}{\partial t}+j\frac{1}{2}\beta_{2\kappa}\frac{\partial^2 A_\kappa}{\partial t^2}=-\frac{\alpha_\kappa^{(prop)}}{2}A_\kappa-\frac{1}{2}\alpha_\kappa^{(FCA)}A_\kappa-\beta^{(TPA)}f_{\kappa,2}\left|A_2\right|^2A_\kappa+\\
&-\beta^{(TPA)}f_{\kappa,1}\left|A_1\right|^2A_\kappa+j2(1-f_R)\gamma_\kappa\left|A_\mu\right|^2A_\kappa+j2(1-f_R)\gamma_\kappa\left|A_{\mu+1}\right|^2A_\kappa+\\
&+j(1-f_R)\gamma_\kappa\left|A_\kappa\right|^2A_\kappa+j2(1-f_R)\gamma_\kappa\left|A_\nu\right|^2A_\kappa+j\frac{2\pi}{\lambda_\kappa}\Delta n_\kappa A_\kappa+\\
&+j2k_{\kappa,\mu,\mu+1,\nu}A_{\mu+1}A_\mu^*A_\nu e^{j(\beta_{0,\mu+1}+\beta_{0,\nu}-\beta_{0,\mu}-\beta_{0,\kappa})z}+j2k_{\kappa,\mu+1,\mu,\nu}A_\mu A_{\mu+1}^*A_\nu e^{j(\beta_{0,\mu}+\beta_{0,\nu}-\beta_{0,\mu+1}-\beta_{0,\kappa})z}+\\
&+jk_{\kappa,\kappa,\nu,\nu}A_\nu A_\kappa^*A_\nu e^{j(2\beta_{0,\nu}-2\beta_{0,\kappa})z}+j2k_{\kappa,\mu+4,\nu,\mu+5}A_\nu A_{\mu+4}^*A_{\mu+5}e^{j(\beta_{0,\nu}+\beta_{0,\mu+5}-\beta_{0,\kappa}-\beta_{0,\mu+4})z}+\\
&+j2k_{\kappa,\mu+5,\nu,\mu+4}A_\nu A_{\mu+5}^*A_{\mu+4}e^{j(\beta_{0,\nu}+\beta_{0,\mu+4}-\beta_{0,\kappa}-\beta_{0,\mu+5})z}+R_p(z,t)+R_s(z,t)-\frac{\gamma_{\kappa,\kappa}}{\omega_\kappa}\frac{\partial(\left|A_\kappa\right|^2A_\kappa)}{\partial t}
\end{aligned}\tag{1}$$

where $\kappa=3,4$ for quasi-TE and quasi-TM fundamental Stokes pulses and $\kappa=5,6$ state for first order Stokes waves, respectively. In addition, if $\kappa=3,4$, it results $\mu=1$ and $\nu=4,3$, while if $\kappa=5,6$, it results $\mu=3$ and $\nu=6,5$. Meaning of all terms and other details of complete mathematical model can be found in our recent work [3]. The efficiency of Raman amplification depends on total loss coefficient $\alpha_i^{(tot)} = \alpha_i^{(prop)} + \alpha_i^{(FCA)}$, where $\alpha_i^{(FCA)}$ is the free carrier absorption (FCA) contribution and $\alpha_i^{(prop)}$ is the propagation loss coefficient in the waveguide, depending on material absorption evaluated for the SOI waveguide as [2]:

$$\alpha_i^{(prop)} = \Gamma_{Si}\alpha_{Si}^{(bulk)} + \Gamma_{SiO_2}\alpha_{SiO_2}^{(bulk)} \tag{2}$$

being $\alpha_{Si}^{(bulk)}$ and $\alpha_{SiO_2}^{(bulk)}$ the bulk absorptions of silicon and silica, respectively, and Γ_{Si} and Γ_{SiO_2} the guided-power fractions into silicon and silica, respectively. Eq. (2) suggests that a silicon rib-membrane waveguide, as shown in Fig. 1, could guarantee a significant reduction of optical loss because of absence of any silicon oxide layer. The waveguide is characterized by total rib height H, slab height H_s, rib width W and air cavity H_m.

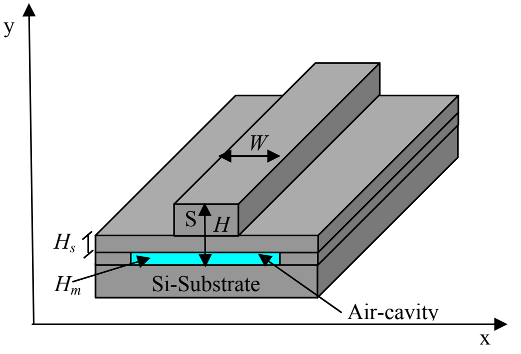

Fig. 1. Schematic diagram of suspended-membrane rib waveguide.

Numerical Results

In the optimization of membrane waveguides, the cavity thickness H_m plays a fundamental role. In fact, it must to be large enough to avoid the slot effect into the air layer, but not too much for structural reasons. Fig. 2(a-b) shows the electric field dominant components by full-vectorial finite element method (FEM) [4] for quasi-TE and quasi-TM polarizations, respectively, at λ = 1.55 μm assuming H_m = 50 nm, H = 400nm, W = 400 nm and $r = H/H_s$ = 0.25. For high index contrast interfaces, Maxwell's equations state that, to satisfy the continuity of electric flux density normal component, the corresponding electric field (E-field) must undergo a large discontinuity with much higher amplitude in the low-index material. Thus, thin air cavities induce strong enhancement of light confinement for vertical component of electric field (quasi-TM mode in Fig. 2(b)), compromising Raman amplification in rib waveguides for quasi-TM modes. Fig.3 shows the propagation loss versus parameter H_m for both polarizations, in cases of membrane and SOI rib waveguides. The curves have been obtained by Eq. (2), in which the guided-power fraction in each layer has been again evaluated by FEM, with at least 60,000 mesh elements, λ = 1.55 μm, H = 400 nm, and

W = 400 nm. In addition, we have considered $\alpha_{Si}^{(bulk)}$ and $\alpha_{SiO_2}^{(bulk)}$ equal to 1dB/cm (worst case in [2]).

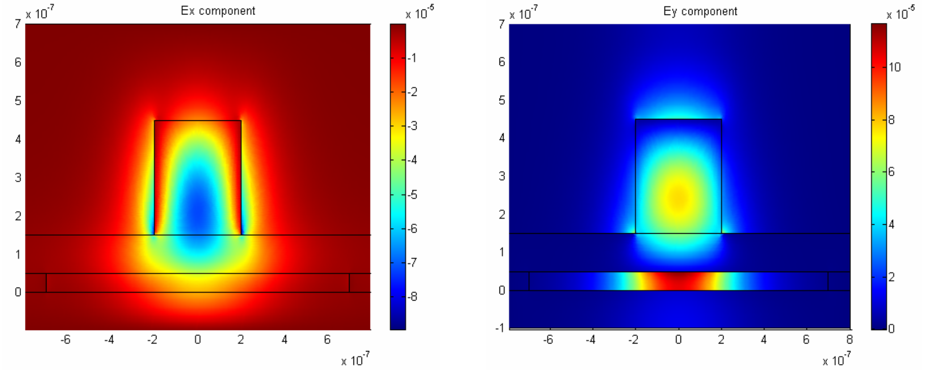

(a) (b)

Fig. 2. Electric field distribution: (a) x-component (quasi-TE mode); (b) y-component (quasi-TM mode).

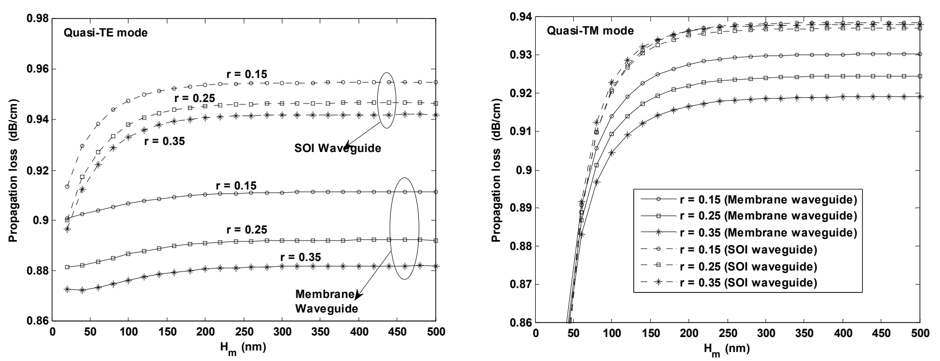

(a) (b)

Fig. 3. Propagation loss versus H_m for various values of r and for silicon membrane and SOI waveguides: (a) quasi-TE mode; (b) quasi-TM mode.

For both polarizations, the membrane waveguide shows a propagation loss smaller than standard SOI rib waveguide. Moreover, r strongly influences the membrane waveguide with respect to SOI one. In addition, for the quasi-TM modes the curves show a large slope for small values of H_m, as due to light confinement into air cavity (see Fig. 2(b)). The presence of air cavity also influences the dispersion properties of the rib waveguide. Fig. 4 shows the group velocity dispersion (GVD) coefficient spectra for membrane and SOI rib waveguides and both polarizations. The simulations are obtained with H_m=200 nm, H=400nm, W = 400 nm, and r = 0.25. The membrane waveguides clearly lead to obtain larger GVD coefficients in the anomalous region for both polarizations with respect to SOI waveguides.

Finally, Fig. 5 shows the net Raman gain versus input pump pulse FWHM width, by solving the system of partial differential equations (1) and comparing membrane and SOI rib waveguides. The input pulse is considered aligned as a quasi-TE mode, while both polarizations of Stokes waves are included, with pump peak power $P_0 = 1$ W, pump wavelength λ_p = 1.434.4µm, Raman gain $g_R = 10.5$ cm/GW [1], and keeping the fundamental Stokes probe power 10 dB below the pump. All optical parameters are calculated by FEM. For both membrane and SOI rib waveguides, the curves related to quasi-TE and quasi-TM modes cross each other for a particular value of FWHM width, namely $\overline{T}_{FWHM}$.

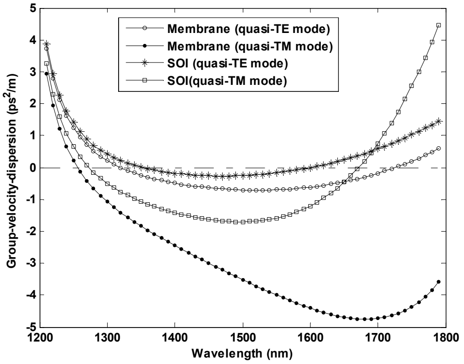

Fig. 4. Group velocity dispersion spectrum

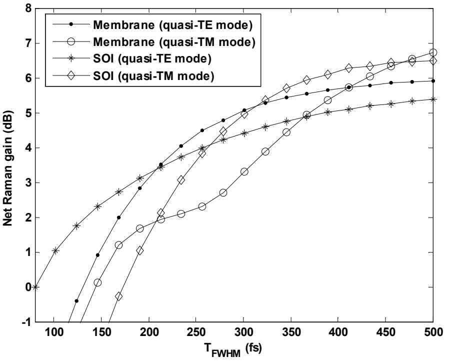

Fig. 5. Raman net gain versus FWHM width

Thus, for both SOI and membrane rib waveguides, when $T_{FWHM} \le \overline{T}_{FWHM}$, quasi-TE modes experience a larger net gain with respect to quasi-TM ones, which have a larger anomalous GVD effect for the designed waveguide. However, the opposite behaviour is revealed for $T_{FWHM} > \overline{T}_{FWHM}$. In fact, larger values of FWHM width induces the quasi-TM dispersion length to be larger than the waveguide length. In this situation, the anomalous GVD effect is not dominant even for quasi-TM modes and then the net gain for TM polarization can increase, becoming larger than for quasi-TE because of its smaller optical mode area. It is worth to note that, if the anomalous GVD effect is not dominant, the membrane waveguides show their advantage in terms of larger net Raman gains with respect to standard SOI waveguides. Our investigations indicate that in dependence of designed cross section, it is possible to find a range of FWHM time widths for which the membrane waveguide shows a larger Raman net gain than SOI waveguide, for both polarizations. This offers the possibility to downscale the waveguide sizes in Silicon Photonics. Moreover, membrane waveguides could induce significant advantages in terms of sizes and power consumption even for SRS effect applied in mid-IR wavelength region.

References

[1] B. Jalali, V. Raghunathan, R. Shori, S. Fathpour, D. Dimitropoulos, and O. Stafsudd, "Prospects for Silicon Mid-IR Raman Lasers", *IEEE J. Sel. Top. in Quantum Electron.*, vol. 12, pp. 1618-1627, 2006.

[2] R. A. Soref, S. J. Emelett, and W. R. Buchwald "Silicon waveguided components for the long-wave infrared region," *J. Opt. A: Pure Appl. Opt.,* vol. 8, pp. 840-848, 2006.

[3] F. De Leonardis and V. M. N. Passaro, "Ultrafast Raman Pulses in SOI Optical Waveguides for Nonlinear Signal Processing", *IEEE J. Sel. Top. in Quantum Electron.*, to be published.

[4] Comsol Multiphysics by COMSOL AB, single license, 2005.